Received: 19 November 2021 | Revised: 27 January 2022 | Accepted: 8 February 2022

DOI: 10.1002/mp.15556

TECHNICAL NOTE

MEDICAL PHYSICS

Technical note: Temperature and concentration dependence of water diffusion in polyvinylpyrrolidone solutions

Ghoncheh Amouzandeh | **Thomas L. Chenevert** | **Scott D. Swanson** | **Brian D. Ross** | **Dariya I. Malyarenko**

Department of Radiology, University of Michigan, Ann Arbor, Michigan, USA

Correspondence
Thomas L. Chenevert, University of Michigan Hospital, 1500 E. Medical Center Dr.,UH B2 room A209L,Ann Arbor, MI 48109-5030, USA.
Email: tlchenev@umich.edu

Funding information
NIH, Grant/Award Numbers: U01 CA166104, U24 CA237683, R35 CA197701, R01 CA190299

[Correction added on 16 Mar, 2022 after first online publication: grant number is updated in acknowledgment section.]

Abstract

Objective: The goal of this work is to provide temperature and concentration calibration of water diffusivity in polyvinylpyrrolidone (PVP) solutions used in phantoms to assess system bias and linearity in apparent diffusion coefficient (ADC) measurements.

Method: ADC measurements were performed for 40 kDa (K40) PVP of six concentrations (0%, 10%, 20%, 30%, 40%, and 50% by weight) at three temperatures (19.5°C, 22.5°C, and 26.4°C), with internal phantom temperature monitored by optical thermometer (±0.2°C). To achieve ADC measurement and fit accuracy of better than 0.5%, three orthogonal diffusion gradients were calibrated using known water diffusivity at 0°C and system gradient nonlinearity maps. Noise-floor fit bias was also controlled by limiting the maximum b-value used for ADC calculation of each sample. The ADC temperature dependence was modeled by Arrhenius functions of each PVP concentration. The concentration dependence was modeled by quadratic function for ADC normalized by the theoretical water diffusion values. Calibration coefficients were obtained from linear regression model fits.

Results: Measured phantom ADC values increased with temperature and decreasing PVP concentration, [PVP]. The derived Arrhenius model parameters for [PVP] between 0% and 50%, are reported and can be used for K40 ADC temperature calibration with absolute ADC error within ±0.016 $\mu m^2/ms$. Arrhenius model fit parameters normalized to water value scaled with [PVP] between 10% and 40%, and proportional change in activation energy increased faster than collision frequency. ADC normalization by water diffusivity, D_W, from the Speedy–Angell relation accounted for the bulk of temperature dependence (±0.035 $\mu m^2/ms$) and yielded quadratic calibration for $ADC_{PVP}/D_W = (12.5 \pm 0.7) \cdot 10^{-5} \cdot [PVP]^2 - (23.2 \pm 0.3) \cdot 10^{-3} \cdot [PVP] + 1$, nearly independent of PVP molecular weight and temperature.

Conclusion: The study provides ground-truth ADC values for K40 PVP solutions commonly used in diffusion phantoms for scanning at ambient room temperature. The described procedures and the reported calibration can be used for quality control and standardization of measured ADC values of PVP at different concentrations and temperatures.

KEYWORDS
ADC calibration, diffusion MRI, diffusion phantom, PVP concentration, temperature dependence

1 | INTRODUCTION

Diffusion weighted imaging (DWI) offers non-invasive insight to tissue microstructure based on self-diffusion of water in biological tissues [1] as an imaging probe that reflects disease presence, progression, or response to treatment.[2–4] Apparent diffusion coefficient (ADC) is a quantitative biomarker derived from DWI[5,6] by fitting a mono-exponential model to signal decay as a function of b-value (diffusion weighting, determined by strength and timings of diffusion-encoding gradients). DW-MRI is a common technique and ADC maps are used for diagnostic and prognostic clinical applications.[2,3,6,7]

Widespread utilization of quantitative DWI in clinical studies at different sites and across multiple platforms requires quality control (QC) assessments for ADC accuracy and reproducibility.[6,8] Sources of technical variability must be characterized and controlled via QC relative to anticipated biologic/therapeutic diffusion changes.[6] Quantitative Imaging Biomarker Alliance (QIBA) metrology guidelines recommend that systematic bias characterization is performed using phantoms with known ADC values.[6,9] Since water mobility is dependent on temperature, knowledge and control of temperature of diffusing media in phantoms are essential in the course of absolute measurements used for technical QC.[10,11] While temperature dependence of ADC is typically not relevant in living tissue due to body temperature regulation, precise knowledge of temperature and water diffusion within polyvinylpyrrolidone (PVP) materials is a prerequisite for calibration of PVP-based DWI phantoms prior to their use in assessment of MRI scanner ADC bias and linearity.

DWI phantoms based on aqueous solutions of PVP provide mono-exponential DWI signal decay with increasing b-value[12,13] and have been used to validate quantitative DWI techniques. PVP solutions are preferred to pure water due to higher viscosity that dampen fluid convection, and their ADC values are tunable by changing PVP concentration to span the ADC range of human tissues. Given an adequate range and known diffusion properties, PVP-based phantoms may be used to assess MR system bias and linearity in ADC measurement,[6,12] since such characterization requires comparison to true diffusivity values.[8]

Given that the water ADC in PVP phantoms depends on polymer molecular weight, solution concentration, and temperature, the issue of water diffusion calibration in PVP solutions has gained attention in recent studies.[14–16] To mitigate temperature dependence of ADC measures, current multi-center QC programs have utilized temperature control of PVP materials using an ice-water bath.[14] Ice-water thermalization when performed properly provides accurate measurements, but requires relatively lengthy phantom preparation.[10,14,17,18] This has limited adoption in the clinical environment since phantom scanning at ambient temperature would offer a more practical advantage. Furthermore, the water diffusion coefficient for 0 to 50% PVP at room temperature spans the full tissue diffusivity range (~0.3 to 2.2 μm^2/ms), whereas at 0°C only half of the range is covered.[14] Assessment of MRI system bias and linearity for ADC beyond 2.2 μm^2/ms is not particularly relevant for human studies. However, ambient temperature diffusion QC protocols require precise knowledge of internal phantom temperature, or addition of an in situ MR-visible thermometer,[11] along with the calibration of ADC values as a function of the given ambient temperature. Scan room temperature can vary across facilities, and a nominal 5°C temperature difference can translate to a large (>15%) phantom ADC variation.

The objective of this study was to investigate the temperature and concentration dependence of ADC for PVP solutions contained in the QIBA/NIST phantom over the scanner room temperature range to provide ground truth ADC values and a calibration equation to facilitate standardization of quantitative DWI measurements for clinical trials across multiple MRI scanner systems.

2 | MATERIALS AND METHODS

2.1 | PVP DWI phantom and temperature control

This study used a commercially-available (Caliber MR, Boulder, CO) QIBA/NIST diffusion phantom design containing an array of thirteen 20 ml vials with PVP-concentrations of 0%, 10%, 20%, 30%, 40%, and 50% w/w of 40 kilo-Dalton (K40) polymer moiety in a spherical polyacrylic shell.[14]

Phantom DWI scans were performed at three room temperatures by setting the scan room thermostat to low, mid, and high settings. After the scan room equilibrated at a given setting, air temperature in the bore was noted and water at that temperature was used to fill the phantom shell. The phantom was then allowed to equilibrate in the bore for additional 3 h. Internal phantom temperature was monitored using an MRI-safe fiber optic temperature probe (OPSENS OPT-M model, Quebec, CA) with ±0.1°C accuracy. Temperature monitoring confirmed the thermal equilibrium during DWI data acquisitions at (19.5, 22.5, 26.4) ± 0.2°C.

2.2 | DWI acquisition and gradient calibration

Scans were performed on a clinical 3T scanner (Philips Ingenia sw v5.4, Best, Netherlands) with the phantom positioned at the magnet isocenter in the head coil. DWI acquisition parameters were: single-shot spin-echo echo-planar imaging (EPI) with parallel imaging (SENSE) factor = 2; TR/TE = 4000 ms/120 ms; FOV = 200 mm × 200 mm and 1.5 × 1.5 × 5.0 mm^3 acquired voxels; three 5 mm slices with a 0 mm gap centered on PVP tubes; 11 nominal b-values = 0, 250, … 2500 s/mm^2 along three orthogonal axes (i.e., X, Y, and Z in magnet frame), and repeated as 10 dynamics, where each loop through all b-values and directions required 4 min 8 s. The TE was sufficiently short for the long-T2 PVP,[19] and constant TR over all b-values with dynamic averaging suppressed potential T1-bias. DWI for each direction, b-value, and dynamic were stored as separate images to facilitate inspection for drift or artifact prior to averaging, and to allow signal-to-noise-ratio (SNR) calculation[20] in subsequent processing.

To increase ADC measurement accuracy, a gradient calibration step (described in Supporting Information) based on known ice–water diffusion coefficient[21] was performed for each gradient channel used to encode diffusion. The measured b-value correction factors between 0.5% and 4% dependent on b-value and gradient-direction (Figure S1) were then applied to nominal b-values for ambient temperature ADC calculation. The trace-DWI were formed by geometric average of individual DWI directions, and direction-average b-value calculated after gradient calibration. The system gradient-nonlinearity (GNL) maps were constructed for direction-average b-values using vendor-provided GNL characteristics.[22] The predicted b-value bias was between −0.47% and 0.92% for phantom vials within 6 cm of isocenter (Figure S2). The spatial GNL correction was then applied to calibrated gradient direction-average b-values (Figure S2) to achieve <|0.5|% GNL bias for the ADC measurements.

2.3 | PVP phantom ADC analysis

A mono-exponential diffusion model was used to derive phantom ADC maps:

$$S_b = S_0 \times \exp(-\mathrm{ADC} \times b) \quad (1)$$

To limit the ADC model fit bias due to the noise-floor to below 0.5%, the maximum b-value for the fit was determined by simulations (Figure S3). Briefly, DWI SNR was estimated by signal temporal mean and variance over the 10 dynamic DWI scans calculated on a pixel-by-pixel basis.[20] This SNR was used to estimate noise-floor bias in ADC measurement via Monte-Carlo simulations as a function of b-value range and true diffusion between 0.25 and 2.5 μm^2/ms (Figure S3).

Room temperature PVP ADC calculation was then performed for trace-DWI over the range of b-values between 0 and b_{max}, where b_{max} varied with PVP concentration: b_{max} = 1000, 1250, 1500, 2250, 2500, 2500 s/mm^2 for [PVP] = 0%, 10%, 20%, 30%, 40%, 50%, respectively. After reconstructing ADC maps using calibrated b-values over sample-specific b-value ranges, 3D Slicer (v4.6.2) was used to extract mean values from VOIs manually placed on central six vials (Figure S2). Only the central vial was used for [PVP] = 0%. The VOIs varied from 7 to 17 cm^3 to exclude visible artifacts.

2.4 | ADC(T) calibration

The temperature dependence of VOI-mean water ADC in PVP was fit by Arrhenius model:[15,21,23]

$$\mathrm{ADC} = \mathrm{A} \times \exp(-E_a/RT) \quad (2)$$

where A (mm^2/s) is the diffusion coefficient in the limit of infinite temperature also termed "collision frequency" factor, E_a (kJ/mol) is the activation energy for translational diffusion of water molecules; R (kJK^{-1} mol^{-1}) is the universal gas constant, and T is the absolute temperature in Kelvin (K). Linear regression fitting of log-ADC(μm^2/ms) versus inverse temperature, T (K), for individual PVP solutions was performed based on the equation:

$$\log(\mathrm{ADC}) = \mathrm{C1} + \mathrm{C2} \times \left[\frac{1000}{T}\right] \quad (3)$$

The calibration coefficients, C1 and C2, and their corresponding standard error of the fit were tabulated for studied PVP solutions and temperatures between 19°C and 26°C. The resulting calibrations were compared to previously reported in the literature for K40[15,24,25] and different polymer moieties K30, K90[15,16] in Supporting Information.

2.5 | Arrhenius parameter [PVP] dependence analysis

The Arrhenius model parameters were derived from calibration constants as:

$$E_a = \mathrm{C2} \times R; \quad A = \exp(\mathrm{C1}), \quad (4)$$

and their confidence intervals obtained by error propagation from C1 and C2 fit errors. The concentration dependence of Arrhenius model parameters was

modeled by linear relation between 0% and 40% [PVP] with intercepts fixed to water E_W and A_W values, respectively:

$$A = A_W + K_A \times [PVP]\,;\; E_a = E_W + K_E \times [PVP] \quad (5)$$

Further characterization of concentration dependence relative to well-established water values (from Speedy–Angell (SA) relation[21,26]) was explored for normalized A_{PVP}/A_W and ($Ea_{PVP} - Ea_W$) Arrhenius parameters versus [PVP] <40%. Linear models of these normalized Arrhenius parameters were constrained to intersect $(A_{[PVP]=0}/A_W) = 1$ and $(Ea_{[PVP]=0} - Ea_W) = 0$:

$$\frac{A_{PVP}}{A_W} = K_{AW} \times [PVP] + 1; \quad E_{PVP} - E_W = K_{EW} \times [PVP] \quad (6)$$

2.6 | ADC([PVP]) calibration

Finally, to isolate ADC dependence on PVP concentration from temperature dependence of water diffusion, ADC in PVP at all measured temperatures were normalized by pure water diffusivity via well-established Speedy–Angell,[21,26] D_W, at the corresponding temperatures and fit to a quadratic calibration function of %[PVP] with intercept constrained to 1:

$$\frac{ADC_{PVP}}{D_W} = K_1 \times [PVP]^2 + K_2 \times [PVP] + 1. \quad (7)$$

The PVP concentration dependence model derived from this work was compared to NIST measurements[19] and previously reported ADC values[24,25] for K40 water solutions studied across four scanner systems, as well as for K30 and K90 PVP moieties.[15,16] The overall calibration accuracy was estimated by the difference between calibrated and measured ADC.

All described analysis was performed in MATLAB R2019b (The Mathworks, Inc., Natick, MA), using "*lscov*" function for linear regression model fit and parameter error estimate.

3 | RESULTS

Figure 1a shows the middle slice through the phantom representing the position and [PVP] of each vial with Figure 1b showing the corresponding ADC map for that slice. Measured ADC values decreased with increasing PVP concentration and decreasing temperature as summarized in Table 1. Plots of log(ADC) versus inverse temperature in Figure 1c illustrate Arrhenius model fit (Equations (2) and (3)) used to derive calibration coefficients, C1 and C2, by linear regression (Equation (3)).

TABLE 1 Mean ADC values ± standard deviation in units of μm^2/ms for water and five PVP concentrations (w/w) at three measured temperatures

[PVP]	19.5°C	22.5°C	26.4°C
0%	1.975 ± 0.004	2.131 ± 0.003	2.346 ± 0.004
10%	1.545 ± 0.005	1.672 ± 0.006	1.853 ± 0.007
20%	1.162 ± 0.003	1.268 ± 0.003	1.426 ± 0.007
30%	0.832 ± 0.003	0.913 ± 0.004	1.036 ± 0.003
40%	0.529 ± 0.002	0.596 ± 0.002	0.673 ± 0.004
50%	0.276 ± 0.005	0.329 ± 0.003	0.383 ± 0.002

TABLE 2 Linear regression fit coefficients ± standard error for log(ADC) dependence on inverse temperature data in Figure 1c based on Equation (3)

[PVP]	C1	C2 (K)
0%	8.09 ± 0.03	−2.17 ± 0.01
10%	8.26 ± 0.10	−2.29 ± 0.03
20%	8.97 ± 0.19	−2.58 ± 0.06
30%	9.28 ± 0.23	−2.77 ± 0.07
40%	9.71 ± 0.56	−3.02 ± 0.17
50%	12.75 ± 1.39	−4.10 ± 0.40

Fit coefficients and their standard errors are reported in Table 2 for each studied PVP concentration. The fit parameter errors are increasing for higher [PVP]. The absolute fit ADC deviation from measured values was within ±0.016 μm^2/ms, and mean absolute calibration error over the full PVP water ADC range was 0.7%. These results can be used for ADC(T) calibration at known [PVP] concentrations according to Equation (3).

Good alignment of current K40 calibration data to 3-year-old multi-site data 0%, 20%, and 40% [PVP],[25] and other previous K40 PVP studies[15,24] at intermediate temperatures is shown in Figure S4a. This figure also illustrates that for intermediate PVP concentrations not directly calibrated in this work, the linear interpolation can be performed between two calibrated values. For instance, for Keenan et al.,[24] 20% PVP values (Figure S4a, cyan asterisks) were derived by linear interpolation of reported ADC results for 18% and 25%.[24] Higher deviation observed for 40% PVP from Keenan et al.[24] (Figure S4a, green asterisks) versus other studies could be due to low b_{max} = 900 s/mm^2 used for the fit that likely limited contrast to noise ratio of derived ADC for this low mobility material.

Figure S4b further compares this K40 study to other available temperature calibrations for K30 and K90 PVP materials, where only lines derived from the fit coefficients are displayed on log(ADC) scale for greater clarity. The observed finite deviations of calibration lines indicate sensitivity to phantom molecular weight, temperature measurement errors, and utilized b-values. For example, dynamic temperature scan in Wagner et al.[16]

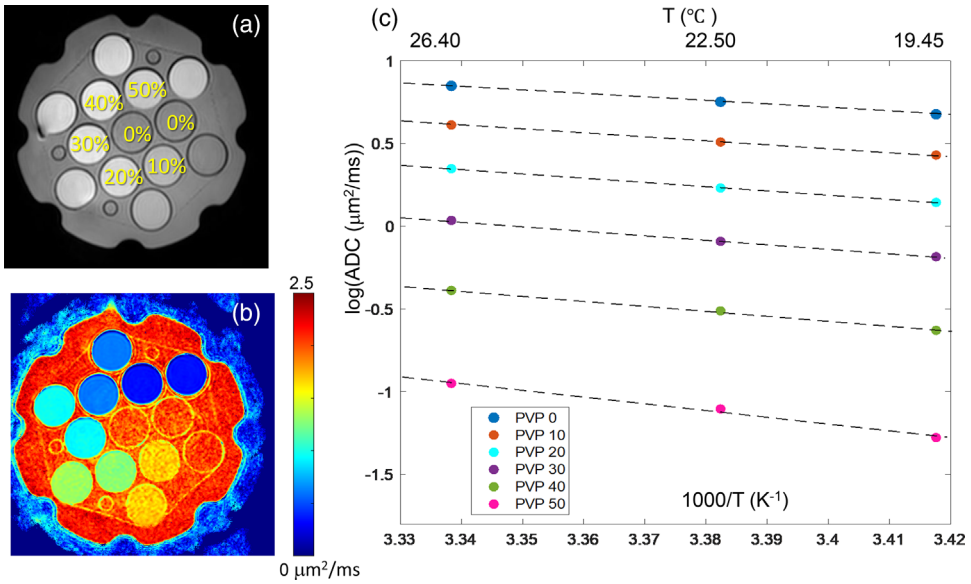

FIGURE 1 QIBA/NIST PVP diffusion phantom (a) MR image illustrating vials' position and PVP %weight/weight concentration. (b) Corresponding ADC map at 26.4°C, and (c) log of ADC values for each PVP concentration (data symbols color-coded in the legend) at three measured temperatures (top axis). Dashed lines display the linear fits to the log(ADC) data as a function of inverse temperature (bottom axis) with the corresponding measured ADC values and fit coefficients summarized in Tables 1 and 2, respectively

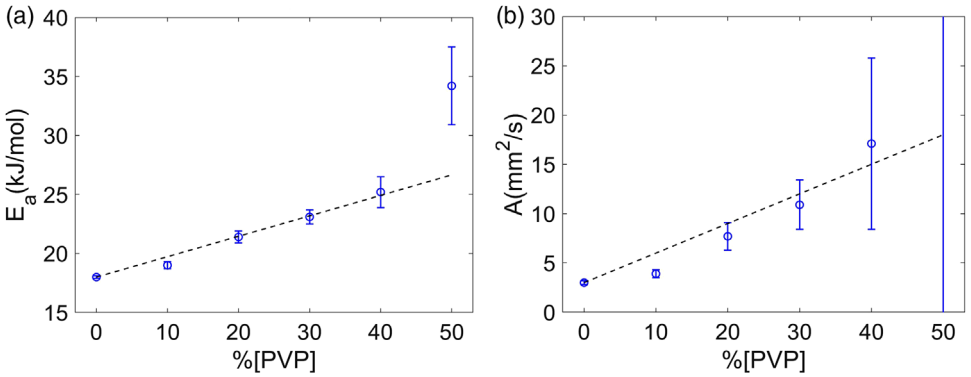

FIGURE 2 Arrhenius model fit parameter values and error bars are shown as a function of %PVP for activation energy, E_a, in (a) and for collision frequency factor, A, in (b). At 50%, A was 350 ±470 mm^2/s (outside of the plot). Dashed lines in both plots show the linear fits based on PVP 10%–40% points with intercept fixed to appropriate water values 3 mm^2/s (for A) and 18 kJ/mol (for E_a) and fit slopes of $K_E = 0.173 \pm 0.007$ (kJ/(mol%)) and $K_A = 0.30 \pm 0.03$ (mm^2/(s%))

showed apparent temperature hysteresis for pure water (Figure S4b, blue) and exhibits the largest deviation from Speedy–Angell calibration (Figure S4b, red)[21] compared to data from Mills[27] (Figure S4b, cyan) and this study (Figure S4b, black dots). The calibration differences are most pronounced for the high [PVP] 50% perhaps due to reduced contrast to noise at $b_{max} = 700$ s/mm^2 used in Wagner et al.[16] versus $b_{max} = 2500$ s/mm^2 used in this study. These results indicate that application of derived calibration constants for ADC(T) may be less accurate in the PVP solution of different molecular weights and at high concentrations.

The Arrhenius model parameters calculated from the corresponding C1 and C2 (Equation (4)) for each PVP concentration are plotted in Figure 2. Fit parameter errors increased with increasing PVP concentration, potentially reflecting reduced contrast-to-noise ratio for the high [PVP] materials. With exclusion of 50% PVP outliers and fixing the intercepts to water parameter values, A and E_a approximately followed linear dependence on the PVP concentration between 10% and 40% as summarized in Table 3. While collision frequency factor A scaled with the PVP concentration (e.g., doubling for 20% vs 10% and 40% vs 20%), the activation energy E_a only increases moderately (from 19 to 25 kJ/mole) for these materials. However, deviations from the linear model in Equation (5) were pronounced particularly for collision frequencies, suggesting limited accuracy of the

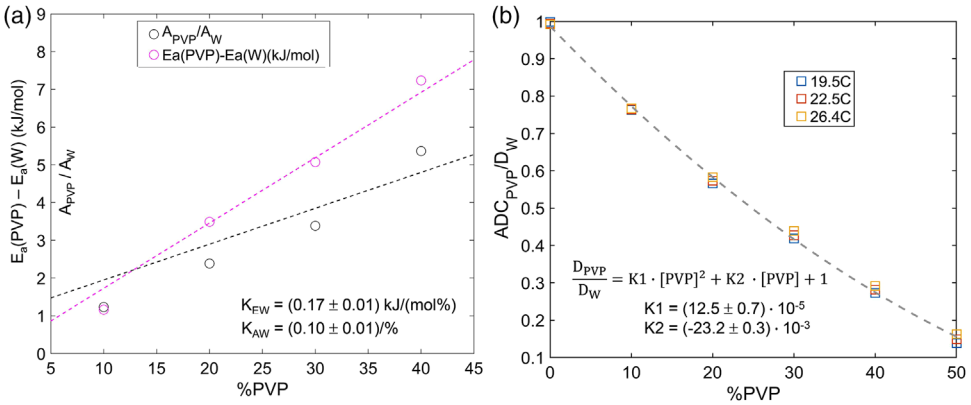

FIGURE 3 Concentration dependence of deviation from pure water (W) values of Arrhenius model fit diffusion parameters (collision frequency, A, and activation energy, E_a) is shown in (a) for 0% to 40% PVP. The vertical axis in (a) is common for difference in activation energies and ratio of collision frequencies relative to pure water. Measured ADC_{PVP} normalized to the theoretical diffusion value of pure water, D_W (calculated from Speedy–Angell relation) is shown in (b) for 0% to 50% PVP and three temperatures color-coded in the legend. Dashed curves show the linear (in a) and quadratic (in b) least squares fit for %PVP dependence over plotted ranges. The fit intercepts were constrained to 1 (for normalized A and ADC) and 0 (for E_a difference), and the fit slopes are listed on the figures

TABLE 3 Derived Arrhenius model parameters ± standard error reported for each PVP concentration

[PVP]	E_a (kJ/mol)	A (mm²/s)
0%	17.99 ± 0.11	3.20 ± 0.15
10%	19.10 ± 0.26	3.94 ± 0.41
20%	21.41 ± 0.45	7.66 ± 1.40
30%	23.06 ± 0.56	10.88 ± 2.47
40%	25.24 ± 1.25	17.12 ± 8.72
50%	34.14 ± 3.33	350.40 ± 474.14

corresponding linear model for the concentration dependence.

Figure 3a further explores concentration dependence of Arrhenius parameters normalized by the corresponding known values of pure water via Speedy–Angell. Higher apparent slope (Equation (6)) of the concentration dependence for relative activation energy (K_{EW} = 0.17 ± 0.01 (kJ/mol%)) versus that of normalized collision frequency (K_{AW} = 0.10 ± 0.01 (1/%)) is consistent with observed reduction of ADC with increasing PVP concentration (Table 1), primarily due to increasing E_a with respect to that of pure water. This figure also highlights limited accuracy of the linear fit models of Equation (6), particularly for normalized collision frequencies, which could lead to the substantial calibration errors for ADC(T) calculation.

As illustrated in Figure 3b, direct normalization of PVP water ADC by the corresponding theoretical pure water SA-values essentially accounts for the bulk of the observed ADC temperature dependence (in Figure 1c). Moreover, these normalized data were reasonably well fit by a simple quadratic function of PVP concentration with only two free parameters (Equation (7): K1 = (12.5 ± 0.7)· 10^{-5} and K2 = (−23.2 ± 0.3)· 10^{-3}), over the full studied concentration range, including [PVP] = 50%. The maximum observed deviations from calibrated ADC values were ±0.035 μm^2/ms at 19°C (for 50% PVP) and 26°C (for 30% PVP). For this proposed quadratic calibration model, the mean absolute ADC error across the studied range of temperatures and PVP concentrations was 2.4%.

Figure S5 shows the summary of available PVP data from published sources and current "UM" study (color-coded in the legend) falling close to the proposed quadratic calibration curve using K1 and K2 values derived exclusively from UM data (Figure S5, dashed). This preliminary analysis suggests the possibility of universal calibration for PVP concentration nominally independent of temperature and PVP molecular weight. Comparable data dispersity for high precision measurements at multiple temperatures (Figure S5a) versus multiple molecular weights and concentrations at a single temperature (Figure S5b) indicates that experimental measurement errors are the likely cause for the observed deviations from the provided calibration curve (Figure S5, dashed).

4 | DISCUSSION

The goal of this study was to provide accurate measurements of ADC values of different PVP concentrations over the range of scanner room temperatures to support quantitative use of PVP-based DWI phantoms. Phantom scanning at ambient temperature is generally more practical for the clinical scanner environment than thermal control via ice-water. Moreover, susceptibility artifacts adjacent to ice-cubes[14] are avoided at room temperature. Assuming K40 phantom temperature is accurately measured within the range of 19–26°C, the estimated ADC values can be directly compared to the look-up table of ADC predicted using calibration

constants from this study to assess system bias and linearity. Such calibration procedure would be limited to the tabulated PVP concentrations, or their linear interpolation. Its accuracy will also depend on the measurement accuracy of provided calibration coefficients and temperatures. Several factors that potentially improve calibration accuracy (mean error of 0.7%) of the current study compared to previous approaches[15,16,24] reduced noise bias depending on maximum b-value used, direction-dependent gradient calibration, and gradient nonlinearity correction.

A two-step alternative procedure is also demonstrated to estimate ADC within the room temperature range for arbitrary K40 PVP concentrations: (1) use well-established water diffusion value at the given temperature via the Speedy–Angell model[21,26]; and (2) scale this by the multiplicative factor, F, where $F = 12.5 \times 10^{-5} \times [\mathrm{PVP}]^2 - 23.2 \times 10^{-3} \times [\mathrm{PVP}] + 1$. Note, even though this multiplicative factor is independent of temperature, one still requires an accurate phantom temperature to properly estimate the pure water diffusivity value.[21] Therefore both methods would rely on an accurate temperature reading (<0.2°C). While temperature measurement is not the focus of this study, promising technology exists[11] that may provide a convenient in situ temperature readout.

Our results show that temperature dependence of pure water diffusion coefficient accounts for the bulk of ADC temperature dependence in PVP solutions. Finite residual dispersion $\mathrm{ADC}_{\mathrm{PVP}}/D_{\mathrm{W}}$ observed over the 19–26°C range could be partly due to experimental measurement error. When normalized by diffusion coefficient of pure water, ADC in PVP solutions followed an apparent quadratic dependence on PVP concentration, largely independent of temperature. Moreover, retrospective inspection of data from all available calibration studies,[15,16,24] including variable molecular weight PVP (K30, K40, and K90), indicated that the quadratic fit coefficients from this study apply remarkably well to all prior data, suggesting PVP ADC normalized to water is not a strong function of PVP molecular weight. This further suggests our proposed normalization procedure, and K1 and K2 values derived from this study have general application for prediction of diffusion in PVP-based phantoms.

As discussed in Holz et al.,[21] self-diffusion of water follows non-Arrhenius behavior in the 5°C to 55°C range; however, over typical room temperatures, the Speedy–Angell (non-Arrhenius) fit shows good agreement to the Arrhenius model. This model also aligned well with the 20% and 40% 40 K PVP results from previous multi-site study[25] and others[15,24] at intermediate temperatures. Based on the Arrhenius model, activation energy and temperature have greater effect on ADC relative to collision frequency factor. Increasing the temperature or decreasing the activation energy would increase the diffusion rate. In water-PVP solutions, collisions with solute particles, hydrogen bonding, and lower solution temperature reduce molecular water displacement and measured diffusion. Increasing the PVP concentration resulted in a steeper increase of activation energy difference from pure water compared to the collision frequency consistent with increased hydrogen bonding[28,29] between water and PVP being the driving factor for observed reduced diffusion in more concentrated solutions.

One limitation of the study is that only three temperatures were used similar to Pullens et al.[15] Thus, results cannot be confidently extrapolated outside of the measured range. Nevertheless, the observed good alignment with previous multi-scanner study at multiple temperatures[25] supports adequate fidelity of the performed calibration. Another limitation is that Arrhenius temperature calibration procedure does not account for concentration dependence and different molecular weights (e.g., K90 vs K30 in Wagner et al.[16]). Furthermore, for specific [PVP] concentrations, temperature calibrations were evidently sensitive to changes in molecular weight over the K30 to K90 range. As illustrated, these limitations could be effectively circumvented for ADC normalization by SA water diffusion coefficient. More comprehensive studies of different molecular weight PVP solutions would be needed to establish accuracy of the proposed universal temperature and concentration calibration of water ADC.

In conclusion, to enable accurate ADC measurements and scanner DWI QC at ambient scan temperatures, precise and accurate calibration of water diffusion in PVP solutions at room temperatures is essential. As such, temperature and concentration dependence of ADC for 0%–50% K40 PVP utilized in QIBA NIST DWI phantoms were studied within typical scan room temperature range and using regression model, yielding a calibration equation for future use. Water diffusion in PVP solutions between 19°C and 26°C was well described by the Arrhenius model. In addition, use of an alternative method to predict ADC as a function of [PVP] scaled to the theoretical diffusivity of water at the given room temperature is also presented and shown to be consistent with prior studied data, nominally independent of temperature and PVP molecular weight.

ACKNOWLEDGMENTS

This work was supported by NIH Grants: U01 CA166104, U24 CA237683, R35 CA197701, R01 CA207290 and R01 CA190299.

CONFLICTS OF INTEREST

The authors have no relevant conflicts of interest to disclose.

REFERENCES

1. Bihan DLe. The 'wet mind':water and functional neuroimaging. *Phys Med Biol.* 2007;52(7):R57-R90.

2. Barkovich EJ, Shankar PR, Westphalen AC. A systematic review of the existing prostate imaging reporting and data system version 2 (PI-RADSv2) literature and subset meta-analysis of PI-RADSv2 categories stratified by gleason scores. *AJR Am J Roentgenol*. 2019;212(4):847-854.
3. Partridge SC, Newitt DC, Chenevert TL, Rosen MA, Hylton NM. Diffusion-weighted MRI in multicenter trials of breast cancer. *Radiology* 2019;291(2):546.
4. Rahbar H, Zhang Z, Chenevert TL, et al. Utility of diffusion-weighted imaging to decrease unnecessary biopsies prompted by breast MRI: a trial of the ECOG-ACRIN Cancer Research Group (A6702). *Clin Cancer Res*. 2019;25(6):1756-1765.
5. Padhani AR, Liu G, Mu-Koh D, et al. Diffusion-weighted magnetic resonance imaging as a cancer biomarker: consensus and recommendations. *Neoplasia*. 2009;11(2):102-125.
6. Shukla-Dave A, Obuchowski NA, Chenevert TL, et al. Quantitative imaging biomarkers alliance (QIBA) recommendations for improved precision of DWI and DCE-MRI derived biomarkers in multicenter oncology trials. *J Magn Reson Imaging*. 2019;49(7):e101-e121.
7. Shenoy-Bhangle A, Baliyan V, Kordbacheh H, Guimaraes AR, Kambadakone A. Diffusion weighted magnetic resonance imaging of liver: principles, clinical applications and recent updates. *World J Hepatol*. 2017;9(26):1081-1091.
8. Raunig DL, Mcshane LM, Pennello G, et al. Quantitative imaging biomarkers: a review of statistical methods for technical performance assessment. *Stat Methods Med Res*. 2015;24(1):27-67.
9. Sullivan DC, Obuchowski NA, Kessler LG, et al. Metrology standards for quantitative imaging biomarkers. *Radiology*. 2015;277(3):813-825.
10. Chenevert TL, Galbán CJ, Ivancevic MK, et al. Diffusion coefficient measurement using a temperature-controlled fluid for quality control in multicenter studies. *J Magn Reson Imaging*. 2011;34(4):983-987.
11. Keenan KE, Stupic KF, Russek SE, Mirowski E. MRI-visible liquid crystal thermometer. *Magn Reson Med*. 2020;84(3):1552-1563.
12. Keenan KE, Ainslie M, Barker AJ, et al. Quantitative magnetic resonance imaging phantoms: a review and the need for a system phantom. *Magn Reson Med*. 2018;79(1):48-61.
13. Pierpaoli C, Sarlls J, Nevo U, Basser PJ, Horkay F. Polyvinylpyrrolidone (PVP) water solutions as isotropic phantoms for diffusion MRI studies. In: Proceedings of the 17th International Society for Magnetic Resonance in Medicine (ISMRM); Honolulu, Hawaii, USA. ISMRM; 2009, p. 1414.
14. Palacios EM, Martin AJ, Boss MA, et al. Toward precision and reproducibility of diffusion tensor imaging: a multicenter diffusion phantom and traveling volunteer study. *AJNR Am J Neuroradiol*. 2017;38(3):537-545.
15. Pullens P, Bladt P, Sijbers J, Maas AIR, Parizel PM. Technical Note: a safe, cheap, and easy-to-use isotropic diffusion MRI phantom for clinical and multicenter studies. *Med Phys*. 2017;44(3):1063-1070.
16. Wagner F, Laun FB, Kuder TA, et al. Temperature and concentration calibration of aqueous polyvinylpyrrolidone (PVP) solutions for isotropic diffusion MRI phantoms. *PLoS One*. 2017;12(6):e0179276.
17. Newitt DC, Tan ET, Wilmes LJ, et al. Gradient nonlinearity correction to improve apparent diffusion coefficient accuracy and standardization in the american college of radiology imaging network 6698 breast cancer trial. *J Magn Reson Imaging*. 2015;42(4):908-919.
18. Malyarenko D, Galbán CJ, Londy FJ, et al. Multi-system repeatability and reproducibility of apparent diffusion coefficient measurement using an ice-water phantom. *J Magn Reson Imaging*. 2013;37(5):1238-1246.
19. Russek SE. *NIST/NIBIB Medical Imaging Phantom Lending Library*. http://doi.org/10.18434/mds2-2366 2021.
20. Dietrich O, Raya JG, Reeder SB, Reiser MF, Schoenberg SO. Measurement of signal-to-noise ratios in MR images: influence of multichannel coils, parallel imaging, and reconstruction filters. *J Magn Reson Imaging*. 2007;26(2):375-385.
21. Holz M, Heil SR, Sacco A. Temperature-dependent self-diffusion coefficients of water and six selected molecular liquids for calibration in accurate H-1 NMR PFG measurements. *Phys Chem Chem Phys*. 2000;2(20):4740-4742.
22. Malyarenko DI, Ross BD, Chenevert TL. Analysis and correction of gradient nonlinearity bias in apparent diffusion coefficient measurements. *Magn Reson Med*. 2014;71(3):1312-1323.
23. Tofts PS, Lloyd D, Clark CA, et al. Test liquids for quantitative MRI measurements of self-diffusion coefficient in vivo. *Magn Reson Med*. 2000;43(3):368-374.
24. Keenan KE, Peskin AP, Wilmes LJ, et al. Variability and bias assessment in breast ADC measurement across multiple systems. *J Magn Reson Imaging*. 2016;44(4):846-855.
25. Malyarenko DI, Swanson SD, Konar AS, et al. Multicenter repeatability study of a novel quantitative diffusion kurtosis imaging phantom. *Tomography*. 2019;5(1):36-43.
26. Speedy RJ, Angell CA. Isothermal compressibility of supercooled water and evidence for a thermodynamic singularity at -45° C. *J Chem Phys*. 1976;65(3):851-858.
27. Mills R. Self-diffusion in normal and heavy-water in range 1-45°. *J Phys Chem*. 1973;77(5):685-688.
28. Gladden JK, Dole M. Diffusion in supersaturated solutions .II. glucose solutions. *J Am Chem Soc*, 1953;75(16):3900-3904.
29. Laage D, Hynes JT. Do more strongly hydrogen-bonded water molecules reorient more slowly ? *Chem Phys Lett*, 2006;433(1-3):80-85.

SUPPORTING INFORMATION

Additional supporting information may be found in the online version of the article at the publisher's website.

How to cite this article: Amouzandeh G, Chenevert TL, Swanson SD, Ross BD, Malyarenko DI. Technical note: Temperature and concentration dependence of water diffusion in polyvinylpyrrolidone solutions. *Med Phys*. 2022;49:3325–3332. https://doi.org/10.1002/mp.15556